ADVANCED FUNCTIONAL MATERIALS
www.afm-journal.de

Correlating Emissive Non-Geminate Charge Recombination with Photocurrent Generation Efficiency in Polymer/Perylene Diimide Organic Photovoltaic Blend Films

Panagiotis E. Keivanidis, Valentin Kamm, Weimin Zhang, George Floudas, Frédéric Laquai, Iain McCulloch, Donal D. C. Bradley, and Jenny Nelson*

Evidence for a correlation between the dynamics of emissive non-geminate charge recombination within organic photovoltaic (OPV) blend films and the photocurrent generation efficiency of the corresponding blend-based solar cells is presented. Two model OPV systems that consist of binary blends of electron acceptor *N′*-bis(1-ethylpropyl)-3,4,9,10-perylene tetracarboxy diimide (PDI) with either poly(9,9-dioctylfluorene-*co*-benzothiadiazole) (F8BT) or poly(9,9-dioctylindenofluorene-*co*-benzothiadiazole) (PIF8BT) as electron donor are studied. For the F8BT:PDI and PIF8BT:PDI devices photocurrent generation efficiency is shown to be related to the PDI crystallinity. In contrast to the F8BT:PDI system, thermal annealing of the PIF8BT:PDI layer at 90 °C has a positive impact on the photocurrent generation efficiency and yields a corresponding increase in PL quenching. The devices of both blends have a strongly reduced photocurrent on higher temperature annealing at 120 °C. Delayed luminescence spectroscopy suggests that the improved efficiency of photocurrent generation for the 90 °C annealed PIF8BT:PDI layer is a result of optimized transport of the photogenerated charge-carriers as well as of enhanced PL quenching due to the maintenance of optimized polymer/PDI interfaces. The studies propose that charge transport in the blend films can be indirectly monitored from the recombination dynamics of free carriers that cause the delayed luminescence. For the F8BT:PDI and PIF8BT:PDI blend films these dynamics are best described by a power-law decay function and are found to be temperature dependent.

1. Introduction

Bulk heterojunctions (BHJ) of donor–acceptor blends have attracted considerable attention as functional layers for flexible, lightweight, and low-cost photovoltaic devices that might serve in the future as power sources for portable electronic products. Reported power conversion efficiencies (PCEs) of polymer/fullerene OPV devices have recently exceeded 8%[1] and are thus approaching the 10% value that is considered necessary for successful commercialization. Other technological targets for device stability and cost of module fabrication will, of course, also need to be met.

For solution-processed organic photovoltaics (OPVs) the best research-cell PCEs have been obtained from devices with photoactive layers consisting of fullerene-based n-type acceptors, namely [6,6]-phenyl-C61 butyric acid methyl ester (PC61BM) and [6,6]-phenyl C-71 butyric acid methyl ester (PC71BM), blended with various p-type polymer donors.[2–4] Despite the impressive progress in PCE values that has been obtained during the last few years, a conclusive picture of the sequence of processes that lead to photocurrent

Dr. P. E. Keivanidis,[+] Prof. D. D. C. Bradley, Prof. J. Nelson
Department of Physics, Blackett Laboratory
Imperial College London
South Kensington Campus, London SW7 2BZ, UK
E-mail: pekeivan@iit.it
Dr. P. E. Keivanidis, Dr. W. Zhang, Prof. I. McCulloch, Prof. D. D. C. Bradley, Prof. J. Nelson
Centre for Plastic Electronics, Blackett Laboratory
Imperial College London, South Kensington Campus
London SW7 2BZ, UK
V. Kamm, Dr. F. Laquai
Max Planck Institute for Polymer Research
Max Planck Research Group for Organic Optoelectronics
Ackermannweg 10, 55128, Mainz, Germany
Dr. W. Zhang, Prof. I. McCulloch
Department of Chemistry
Imperial College London
South Kensington Campus, London SW7 2BW, UK
Prof. G. Floudas
Department of Physics
University of Ioannina
451 10 Ioannina, Greece, Foundation for Research and Technology-Hellas (FORTH-BRI), Greece
[+] Present address: Centre for Nano Science and Technology @Polimi, Istituto Italiano di Tecnologia, Via Pascoli 70/3, 20133 Milan, Italy

DOI: 10.1002/adfm.201102871

generation has not yet been established. Meanwhile, it has become clear[5–7] that photocurrent generation in OPVs can be limited by an unfavourable photoactive layer microstructure for certain systems. This impedes efficient separation of photogenerated interfacial geminate pairs.

For some systems, the geminate pairs form equilibrated charge transfer (CT) states, sometimes termed exciplexes that can be identified by a characteristic CT photoluminescence (PL) band. The CT state energy typically corresponds to the diagonal energy-gap between the frontier orbitals of the donor and the acceptor components of the blend.[8–14] For other systems, a stabilized ground-state CT character has been suggested[15,16] and photocurrent can also be generated after direct excitation of the CT absorption.[17] In fact, the open-circuit voltage (V_{OC}) of OPV cells correlates well with the CT energy absorption of some OPV layers.[18,19] However, the role of CT states for photocurrent generation and the influence of electric field dependent charge separation on the shape of the OPV device current–voltage curve remains controversial.[20–22] CT PL experiments that probe the CT state manifold after thermalisation of the geminate pair and the probability for the activation of CT PL indicate that both appear to be material specific. Recent steady-state PL studies in model OPV blends with increasing CT state energies have shown that the intensity of the CT emission and the efficiency of short-circuit photocurrent generation in the corresponding OPV devices are anti-correlated: as the CT intensity increases, the photocurrent decreases.[23] This observation was assigned to differences in the blend morphology that promotes formation of CT-states and geminate recombination at the expense of free charge-carrier generation. Inconsistent experimental results have been published regarding the effect of externally applied electric fields on the CT luminescence intensity and on the subsequent photocurrent generation efficiency. For polymer/small molecule OPV blends the electric field-induced quenching of steady-state or nanosecond-resolved CT PL does not contribute to either free charge-carrier formation[12] or photocurrent generation.[13] In contrast, a clear correlation has been presented between electric field-induced steady-state CT luminescence quenching and photocurrent generation in polymer/polymer blend-based OPV devices.[24] More recently a report demonstrated an electric field independent photogeneration for a (poly[2,6-(4,4-bis-(2-ethylhexyl)-4H-cyclopenta[2,1-b;3,4-b′]-dithiophene)-*alt*-4,7-(2,1,3-benzothiadiazole)] (PCPDTBT):PC71BM photovoltaic system,[25] while others argued that the current–voltage characteristics of the same system can be described by the Onsager-Braun model assuming field-dependent splitting of interfacial CT-states.[26,27]

There is ongoing development of alternative n-type materials for OPV technologies to substitute the commonly used fullerene-type acceptors.[28–31] One interesting class of these materials is the perylene diimide (PDI) derivatives due to their strong absorption and favourable charge transport properties.[32–37] Steady improvement in the PCE values of organic solar cells based on PDI derivatives has led to a best-to-date PCE of 2.85% for a bulk heterojunction consisting of a benzothiadiazole-containing vinylene compound mixed with a perylene–anthracene diimide electron acceptor.[38–40] Despite this progress in device efficiency, the mechanism of photocurrent generation in PDI-based OPV blends remains less clear than in the case of fullerene-based systems. This is due in part to the fact that fullerenes are pseudospherical geometrical objects, whereas PDI molecules are rigid planar structures that tend to form aggregates and that can readily support the formation of intermolecular excited states, also termed excimers.[29] The impact of the photoactive layer microstructure on photocurrent generation in PDI-based OPV devices seems to deviate from the observations that are generally reported in fullerene-based OPV systems.[41] In particular, the device external quantum efficiency (EQE) of PDI-based photoactive layers does not improve upon increasing the local order of the PDI domains of the blend film.[42] Unlike the case for fullerene-containing solar cells, enhanced packing of the electron acceptor results in a severe reduction of both the exciton dissociation and photocurrent generation efficiencies[42,43] due to exciton and electron confinement in the enlarged PDI domains of the photoactive layer.[32,44] Nonetheless, this observation may be not be applicable to all polymer/PDI composites and the specific polymer–PDI interactions could be tuned by suitable polymeric systems that favor intrafacial mixing.

Recent theoretical studies have suggested that the charge recombination in PDI/polythiophene blends is faster than in fullerene/polythiophene blends.[45] The process of recombination can be radiative even for the case of non-geminate charge recombination.[46,47] Very recently we have shown[17] that PDI-based OPV blends exhibit delayed luminescence in the microsecond timescale. This emission was quenched by the application of a moderate external electric field applied 1 μs after optical excitation. In combination with the sublinear dependence of the CT emission on the excitation intensity,[44] our conclusion was that the CT emission originated from non-geminate recombination, a process that can be suppressed by applying electric fields that promote charge transport to the collection electrodes.

In this work we explore the relationship between the dynamics of the emissive non-geminate charge recombination and the efficiency of photocurrent generation for PDI-based OPV blends, as a function of the photoactive layer structure. For our study we use the PDI derivative (*N*′-bis(1-ethylpropyl)-3,4,9,10-perylene tetracarboxy diimide) as electron acceptor and either poly(9,9-dioctylfluorene-*co*-benzothiadiazole) (F8BT) or poly(9,9-dioctylindenofluorene-*co*-benzothiadiazole) (PIF8BT) as electron donor. The photophysical and the electrical properties of these two PDI-based blends are reported. PDI dispersed in poly(styrene) (PS), a photophysically inactive matrix, was used as a reference for the photophysical studies. The structures of the materials studied are shown in **Scheme 1**.

2. Results

Figure 1 presents the UV-Vis spectra of as-spin-coated and annealed layers of PS:PDI, F8BT:PDI, and PIF8BT:PDI blend films.

For all three systems the emergence of a low-energy absorption band at around 590 nm is observed upon thermal annealing at 90 °C for a period of 30 min in a vacuum oven. This spectral feature has been previously assigned to the formation of well-ordered PDI aggregates in binary-blend polymer/PDI films.[42] Wide-angle X-ray scattering experiments on the F8BT:PDI system

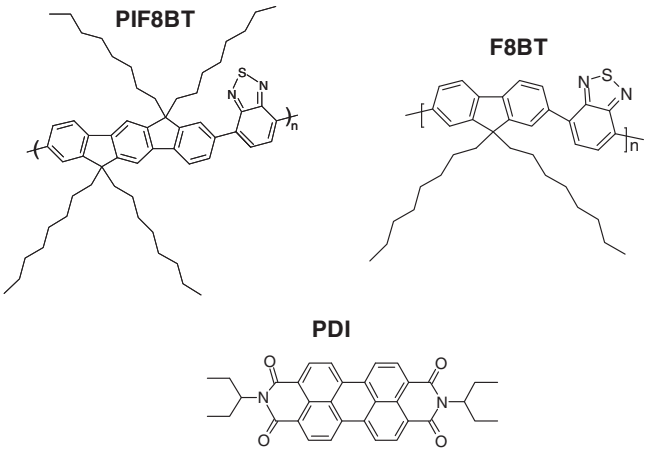

Scheme 1. The chemical structures of the materials used in the study.

(see Supporting Information) further suggest increased order (with a monoclinic unit cell) and the presence of PDI aggregates after thermal treatment. Clearly, both PS:PDI and F8BT:PDI blend films are prone to PDI crystallization upon annealing. In contrast, the PIF8BT:PDI blend film is found less affected by the thermal annealing at this temperature, as indicated by the comparatively small increase in oscillator strength at 590 nm.

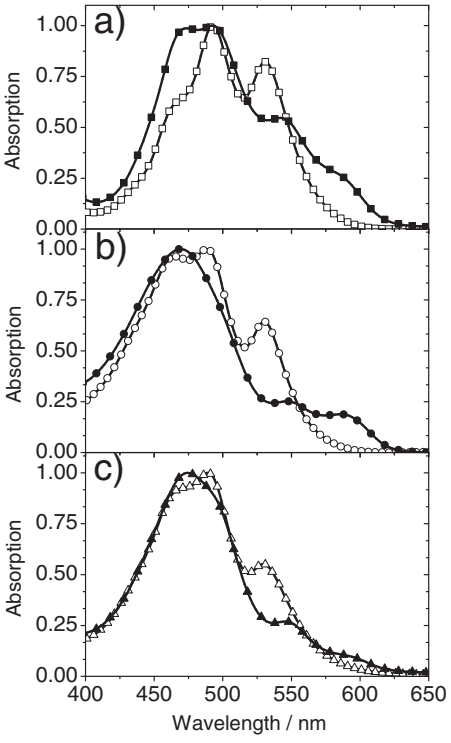

Figure 1. UV-Vis absorption spectra of blend films of: a) as-spin-coated (open squares) and 90 °C annealed (filled squares) PS:PDI; b) as-spin-coated (open circles) and 90 °C annealed (filled circles) F8BT:PDI, and, c) as-spin-coated (open triangles) and 90 °C annealed (filled triangles) PIF8BT:PDI

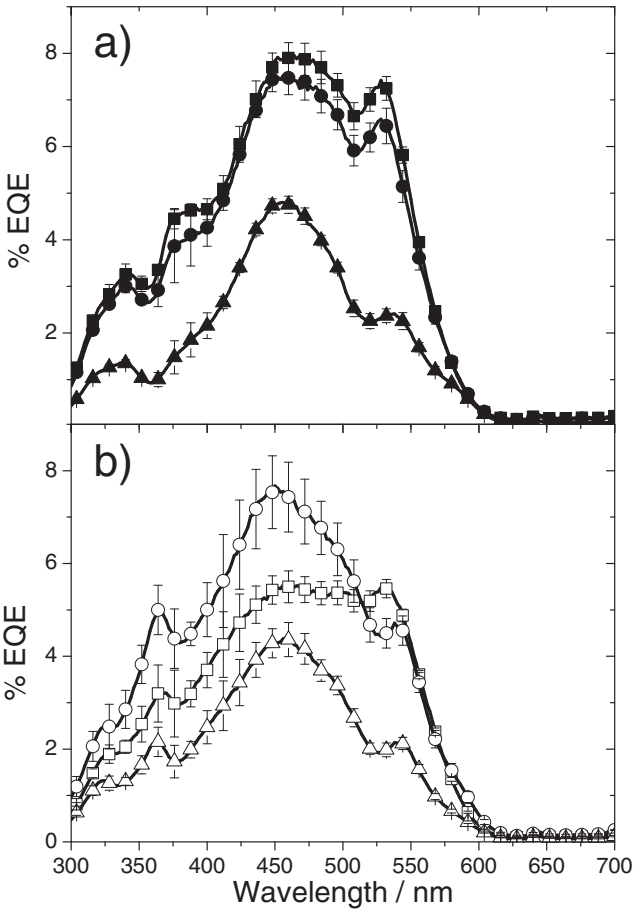

Figure 2. External quantum efficiency (EQE) spectra for: a) F8BT:PDI devices (filled symbols), and, b) PIF8BT:PDI devices (open symbols). In both cases, data are shown for devices with layers as-spin-coated (squares), annealed at 90 °C (circles), and annealed at 120 °C (triangles).

In order to assess the efficiency of photocurrent generation in the OPV binary blends we measured the EQE of a set of F8BT:PDI and PIF8BT:PDI photodiodes. Firstly, we determined the optimum thickness of the active layer that corresponds to maximum photocurrent generation (see Supporting Information). Subsequently, we studied the dependence of the device EQE on annealing temperature.

Figure 2 presents the EQE spectra of the as-spin-coated and annealed F8BT:PDI and PIF8BT:PDI devices.

In agreement with previous observations,[42] thermal treatment negatively impacts the EQE of the F8BT:PDI device, despite the fact the F8BT batch used in this study has a molecular weight that is almost double the one previously used. In contrast, the PIF8BT:PDI device showed an improved photocurrent generation efficiency, when the photoactive layer was annealed at 90 °C. Annealing the PIF8BT:PDI device at 120 °C results, however, in a significant reduction in EQE, as observed for F8BT:PDI devices.

We have previously shown that the efficiency of photocurrent generation in the F8BT:PDI devices is positively correlated to the efficiency of PL quenching of the F8BT:PDI layer.[42] To investigate the reason for the increased EQE of the PIF8BT:PDI

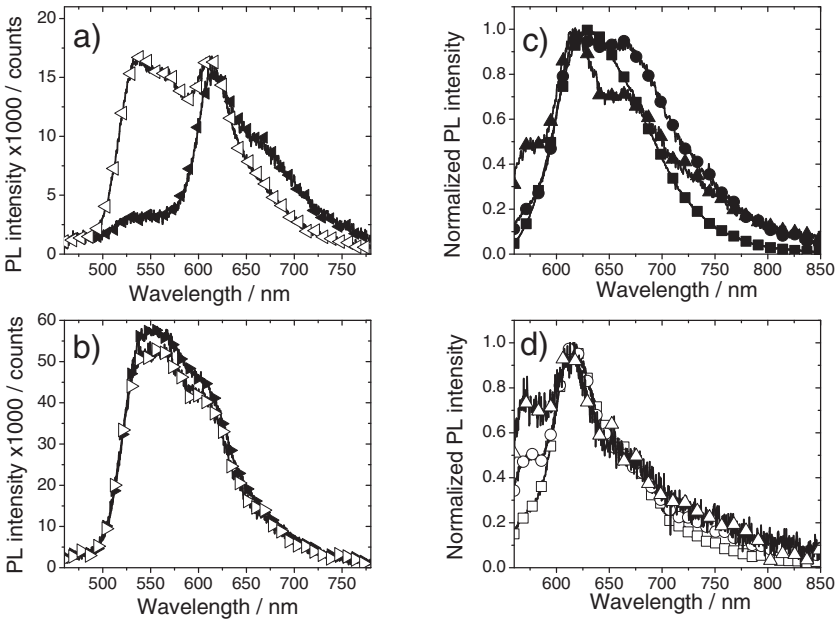

Figure 3. Left side: PL spectra for photoexcitation at 420 nm of: a) as-spin-coated (filled right-triangles) and annealed (open right-triangles) F8BT:PDI, and, b) as-spin-coated (filled left-triangles) and annealed (open left-triangles) PIF8BT:PDI. The spectra are corrected for the absorptance (1–*T*) of the films at 420 nm. Right side: PL spectra for photoexcitation at 530 nm of: c) as-spin-coated PS:PDI (filled squares), F8BT:PDI (filled circles), and PIF8BT:PDI (filled triangles), and, d) annealed PS:PDI (open squares), F8BT:PDI (open circles), and PIF8BT:PDI (open triangles). In all cases films were annealed at 90 °C. All spectra were recorded with 100 ms integration time.

devices after thermal treatment, we performed PL quenching studies on the as-spin-coated and annealed polymer/PDI blend films. For both as-spin-coated and annealed blend films, the PL spectra of F8BT:PDI and PIF8BT:PDI were measured as a function of excitation wavelength. **Figure 3** presents the PL spectra recorded for photoexcitation at 420 nm (Figure 3a,b), in a spectral range where the polymer donor and PDI acceptor both absorb.

Taking into account the absorption strength of F8BT and PIF8BT relative to PDI, we expect that the majority of primary excitations will be formed in the polymer donor component of the blend. We can not exclude however that the PDI component is also directly photoexcited. Previous studies have determined the value of the PLQY efficiency of PS:PDI 60 wt-% to be in the level of 20%,[42] whereas we have determined the PLQY efficiency values of F8BT and PIF8BT used in this study to be 50% and 70%, respectively.

The photoexcitations that are formed in the polymer components can undergo both Förster resonant energy transfer (FRET) and photo-induced charge transfer (PCT) processes with the PDI component. Figure 3a shows that, in the as-spin-coated F8BT:PDI system, the F8BT emission centred at 540 nm is weak compared to the PDI excimer emission at around 620 nm.[42] The vanishing emission of F8BT indicates that the FRET and/or PCT processes is very efficient in the as-spin-coated F8BT:PDI layer. Moreover, the shoulder seen in the spectral region beyond 650 nm indicates the presence of the F8BT-PDI exciplex that emits at 680 nm.[17] In the case of the PIF8BT:PDI system, the PIF8BT emission at 550 nm is the dominant contribution in the PL spectra, whereas the shoulder at 615 nm indicates a weaker PDI emission intensity. Therefore we conclude that in the as-spin-coated blend films the PL quenching of PIF8BT is not as efficient as that of F8BT.

Figure 3a also indicates that thermal annealing was detrimental to the PL quenching of the F8BT component. The PL spectrum of the annealed F8BT:PDI film shows a recovery of the F8BT luminescence in the spectral region below 575 nm. It is also shown that the intensity of the PDI component at 620 nm remains unaffected after annealing, suggesting that thermal treatment of the F8BT:PDI system (at 90 °C) is not affecting the long-range energy transfer from F8BT to PDI, but is only affecting the PCT process that quenches the F8BT exciton. Moreover, the long-wavelength spectral content of the PDI emission sharpens, losing intensity beyond 650 nm, suggesting a reduction in the concentration of the low-energy F8BT-PDI exciplex species after annealing. In contrast, Figure 3b shows that thermal treatment (at 90 °C) of the PIF8BT:PDI blend uniformly decreases the PL intensity of the overall luminescence.

We repeated the PL quenching experiments by exciting the PDI component of the blend films at 530 nm. Under these conditions no energy transfer can take place from the PDI to the polymer matrices. All photoexcitations formed in PDI can now either hole transfer to the polymer components or directly relax to the ground state by radiative and/or non-radiative pathways. Figure 3c,d depicts the 530 nm excited PL spectra of PS:PDI, F8BT:PDI, and PIF8BT:PDI blend films before and after thermal treatment at 90 °C. The spectra comprise a superposition of the PDI excimer luminescence at approximately 610–630 nm[42] and the CT luminescence of the PDI/polymer exciplex[17] at longer wavelengths, peaking around 680 nm.

The PCT-induced PL quenching efficiency (Φ_q) in the F8BT:PDI and PIF8BT:PDI blend films was deduced as previously described, i.e., by comparing the spectral integral of the PDI emission in these two blends with the corresponding spectral integral of PDI in PS:PDI blend films[42] (see non-normalized PL spectra in the Supporting Information). In the case of F8BT:PDI and PIF8BT:PDI as-spin-coated films, the PL quenching efficiencies were found to be Φ_q(F8BT:PDI) = 82% and Φ_q(PIF8BT:PDI) = 86%. After annealing, we determined Φ_q(F8BT:PDI) = 38% and Φ_q(PIF8BT:PDI) = 57%. In the case of the F8BT:PDI system, thermal annealing reduced the spectral width of the CT luminescence band. This reduction was observed to a smaller extent for the PIF8BT:PDI blend film.

We next investigated the relationship between the photophysics of the CT luminescent state and changes in the morphology of the photoactive polymer/PDI blend layers, as inferred from changes in the 590 nm absorption peak of the PDI component. In particular, we performed delayed luminescence

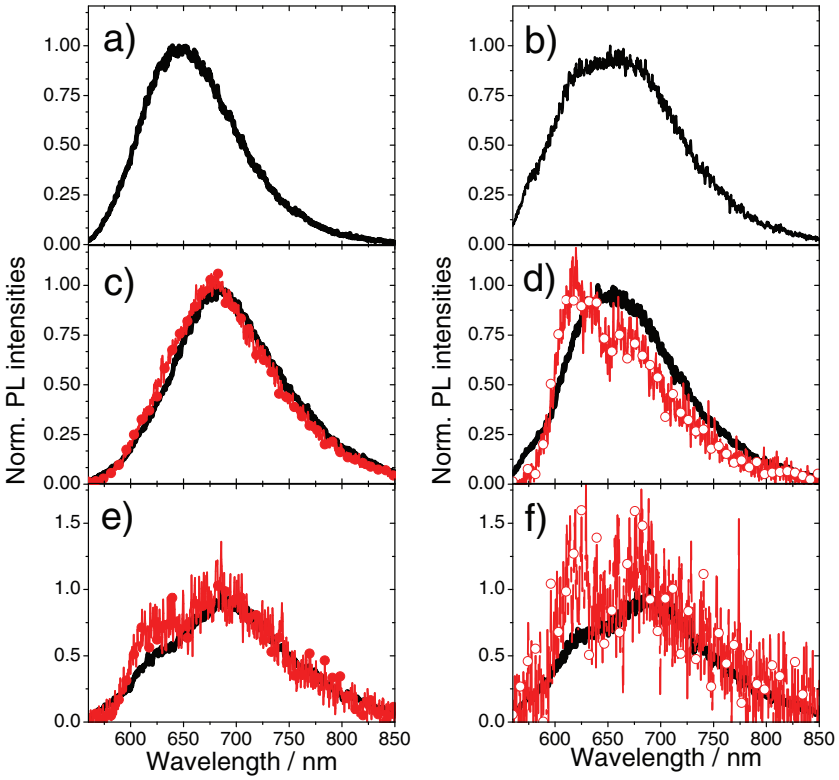

Figure 4. 530 nm excited, time-gated PL spectra for: a) as-spin-coated PS:PDI, b) annealed PS:PDI, c) as-spin-coated F8BT:PDI, d) annealed F8BT:PDI, e) as-spin-coated PIF8BT:PDI, and f) annealed PIF8BT:PDI blend films. For each blend, data are presented at 10 ns after excitation integrated over 10 ns gate time (in black) and at 1 µs after excitation integrated over a 500 ns gate time (in red). No delayed luminescence was detectable in the µs time range for the PS:PDI samples.

experiments (in the microsecond timescale) on the F8BT:PDI and PIF8BT:PDI blend films. For reference purposes we also characterised a PS:PDI blend film. **Figure 4** depicts time-gated PL spectra of as-spin-coated and annealed samples.

PL spectra were recorded for two time regimes, one corresponding to the nanosecond timescale (prompt fluorescence) and one corresponding to the microsecond timescale (delayed luminescence).

No delayed luminescence could be detected for the PS:PDI blend after photoexcitation at 530 nm. The F8BT:PDI and PIF8BT:PDI blend films clearly exhibit the typical red-shifted CT emission at around 680 nm independent of the time domain probed. For the as-spin-coated PIF8BT:PDI blend film (Figure 4e), a residue of the PDI emission was also observed at 620 nm. Thermal annealing of the blend films (Figure 4b,d,f), did not result in spectral changes to the prompt fluorescence spectra. However, obvious differences are observed in the delayed luminescence spectra of the annealed F8BT:PDI system in the microsecond time range. As Figure 4d shows, in the annealed F8BT:PDI blend film the relative intensity of the CT luminescence is significantly reduced whereas the short wavelength region near 620 nm gains PL intensity. For the case of the annealed PIF8BT:PDI blend (Figure 4f) the relative amplitudes of PL in the short and the long wavelength spectral regions remain virtually unaffected.

The delayed luminescence dynamics of the F8BT:PDI and PIF8BT:PDI systems reflect the dynamics of non-geminate charge-carriers that recombine emissively.[17] Therefore, these dynamics can be used as an indirect probe for the efficiency of charge transport in each of the blend layers. The easier the transport of mobile carriers in the layers, the more frequent will be the encounter of non-geminate pairs on the polymer/PDI interfaces for forming the emissive CT species. Consequently the layer that exhibits accelerated exciplex dynamics on the microsecond timescale is expected to also exhibit a better charge transport, which could be beneficial for device structure. **Figure 5** compares the dynamics of the exciplex emission (645–730 nm) of the as-spin-coated F8BT:PDI and PIF8BT:PDI blend films in the microsecond timescale.

For each blend we also measured the decay kinetics for the short-wavelength region (585–640 nm) of the delayed emission spectra in order to look for differences that might arise

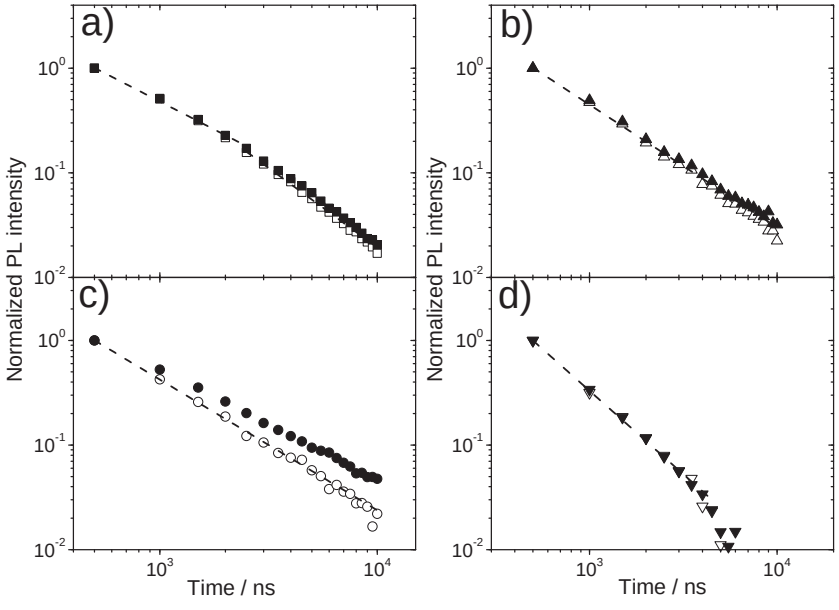

Figure 5. Delayed luminescence decay kinetics in the microsecond timescale for the short (open symbols) and long (filled symbols) wavelength regions of the emission spectra for: a) as-spin-coated F8BT:PDI, b) 90 °C annealed F8BT:PDI, c) as-spin-coated PIF8BT:PDI, and d) 90 °C annealed PIF8BT:PDI blend films. The dash lines are power-law fits to the data (see Table 1 and text for details).

Table 1. Fit exponents of the power-law kinetics for as-spin-coated and 90 °C annealed F8BT:PDI and PIF8BT:PDI blend films. Note that for the as-spin-coated F8BT:PDI blend film a fast and a slow component is identified in the kinetics of both short and long wavelength regime. The corresponding device EQE_{max} values, from Figure 2, are also given.

Blend Film Structure	Power law exponent [585–640 nm]	Power law exponenent [645–730 nm]	EQE_{max} [%]
As-spin-coated F8BT:PDI	–1.07 ± 0.04/ –1.52 ± 0.02	–1.02 ± 0.04/ –1.48 ± 0.02	7.98 ± 0.31
90 °C annealed F8BT:PDI	–1.17 ± 0.01	–1.12 ± 0.01	7.54 ± 0.40
As-spin-coated PIF8BT:PDI	–1.25 ± 0.01	–1.00 ± 0.01	5.55 ± 0.33
90 °C annealed PIF8BT:PDI	–1.60 ± 0.02	–1.57 ± 0.01	7.67 ± 0.69

from the recombination of charges in isolated PDI domains that would lead to delayed emission via re-population of the emissive state of the PDI excimer.[48] Fitting of the obtained decay dynamics in the time range from 500 ns to 10 μs was performed using a power law of the form $I(t) \propto t^{-\alpha}$.[49,50]

Table 1 summarizes the values of the exponent α of the power-law fits, as determined for both the short- and long-wavelength regions of the delayed luminescence spectra of as-spin-coated and annealed F8BT:PDI and PIF8BT:PDI blend films. To link the emissive charge recombination dynamics with the photocurrent generation of each system, the maximum EQE values are also presented for the corresponding devices. Particularly for the as-spin-coated F8BT:PDI film, the decay kinetics of both the short- and the long-wavelength spectral region exhibit two components of a slow and a fast recombination.

3. Discussion

From the above it is clear that thermal annealing has a different impact on the photophysical properties of PIF8BT:PDI and F8BT:PDI blend films and the photocurrent generation efficiency of their corresponding photodiodes. We assign the annealing-induced changes in the photophysical properties of the two systems to differences in the changes that take place in their blend structure after thermal treatment; these are the changes in the phase segregation of the blend components, in the increased long-range order of the PDI domains and in the quality of the polymer/PDI interfaces.

The weak increase in the intensity of the 590 nm absorption peak in the the UV-Vis spectra of the annealed PIF8BT:PDI blend film (Figure 1c) clearly indicates that, unlike the case of the F8BT:PDI blend, thermal annealing of PIF8BT:PDI does not promote extensive formation of well-ordered, phase-separated PDI aggregates. The different behaviour of the two blends upon thermal annealing is likely to result from the different thermal and structural properties of the F8BT and PIF8BT polymers.[42] The magnitude of the thermally induced PDI crystallization in the two blends also influences the impact of thermal treatment in the PL quenching of the films, for both cases where optical excitation was at 420 nm or at 530 nm.

In the case of the 420 nm photoexcitation (Figure 3a,b) the results show that in contrast to the F8BT:PDI blend case, thermal annealing of the PIF8BT:PDI blend results in a reduction of the PIF8BT PL intensity. Therefore, thermal treatment enhances the quenching of the PIF8BT excitons, suggesting that after annealing a larger fraction of the PIF8BT excitons dissociates efficiently at the PIF8BT/PDI interfaces. The increased PL quenching of PIF8BT in the annealed PIF8BT:PDI film is in line with the increased EQE of the corresponding PIF8BT:PDI device. The observed increase in EQE (Figure 2b) takes place in the spectral range that corresponds to the spectral region of the PIF8BT absorption.[17] We interpret this observation as evidence that thermal annealing improves the quality of the PIF8BT/PDI interfaces where the PIF8BT excitons can dissociate more efficiently. In the case of the PIF8BT matrix, thermal annealing at 90 °C may optimize the electronic interaction of PIF8BT and PDI in their interface through a better electronic wavefunction overlap. We exclude the option that the increased EQE in this spectral region is a result of an increase in the absorption strength of the annealed PIF8BT:PDI film. Only a marginal increase (2%) in the optical density at 475 nm was seen in the annealed film of PIF8BT:PDI, in respect to the non-annealed film (not shown).

For optical excitation at 530 nm, the PCT-induced PL quenching efficiency (Φ_q) is found to be reduced in both PIF8BT:PDI and F8BT:PDI systems after annealing, but the reduction is smaller in the case of the PIF8BT:PDI blend. The relatively small increase in the UV-Vis absorption of the annealed PIF8BT:PDI blend films at 590 nm indicates that even after thermal treatment at 90 °C the optimum blending of the PIF8BT and PDI components is maintained in the layer structure of the PIF8BT:PDI system.

In contrast, thermal annealing of the F8BT:PDI layer results in a reduction of the F8BT/PDI interface area due to the demixing of the F8BT and PDI component that is driven by the coalescence of PDI into larger and better ordered grains.[51] The thermally induced PDI crystallization in the F8BT:PDI layer results in a large reduction of the PL quenching, for both excitation wavelengths of 420 and 530 nm, and in a reduced device EQE.

We now focus attention on the delayed luminescence spectroscopic data of Figure 4 and discuss the possibility for correlating the process of emissive non-geminate recombination and the strength of the concomitant polymer/PDI exciplex emission with the efficiency of photocurrent generation. The quality of the polymer/PDI interface in the studied systems not only influences the efficiency of prompt dissociation of excitons that are initially formed in the polymer and PDI domains but also affects the efficiency of the emissive non-geminate charge recombination at this interface. Concurrently, we expect that the system with the most optimized polymer/PDI interfaces will exhibit not only a higher photocurrent generation device efficiency but also a higher exciplex strength that will be activated by non-geminate recombination in the microsecond timescale.

In our discussion we define the exciplex strength as the relative ratio between the delayed luminescence intensities of the exciplex (680 nm) and PDI (630 nm) species in Figure 4. Both emissive species are observed in the microecond timescale in the spectra of the F8BT:PDI and PIF8T:PDI systems as the

products of emissive non-geminate recombination. The exciplex delayed PL emission is generated by the one-step diagonal recombination of the non-geminate pair at the polymer/PDI interface. In contrast, the PDI delayed emission is generated by a two-step mechanism that involves i) the thermally activated back hole-transfer from the $HOMO_{F8BT}$ to the $HOMO_{PDI}$, and, ii) the emissive recombination of the regenerated PDI excited state. High exciplex strength is implied by the dominance of the one-step mechanism when the quality of the polymer/PDI interface is optimum.

Figure 4c,e shows that the exciplex strength of the as-spin-coated blend films in the microsecond timescale is higher for the F8BT:PDI than in the PIF8BT:PDI system. This finding is in agreement with the trend seen in the EQEs of the as-spin-coated F8BT:PDI and PIF8BT:PDI devices. From Figure 2,3 we have found that thermal treatment severely affects the interfaces and the EQE of the F8BT:PDI blend film but not those of the PIF8BT:PDI blend film. Accordingly, the delayed luminescence spectra in the microsecond timescale exhibit a strong reduction of the exciplex strength for the case of the F8BT:PDI system but not for the case of the PIF8BT:PDI system. Therefore delayed luminescence spectroscopy further confirms that the layer structure of the annealed PIF8BT:PDI systems maintains a good mixing of the PIF8BT and PDI components. We note that thermal annealing could possibly alter the exciplex strength in the F8BT:PDI and PIF8BT:PDI blends by differently influencing the non-radiative recombination rates of the CT state and the PDI state in each system. We exclude this option based on the results shown in Table 1. We found that after the thermal annealing of the F8BT:PDI and PIF8BT:PDI layers, the kinetics of the PDI (short wavelength) and the CT emission (long wavelength) peaks change in similar fashion, excluding the possibility that the exciplex strength of each system is affected by different changes in the non-radiative recombination upon annealing.

We now discuss the correlation between the non-geminate recombination dynamics (Figure 5) and the photocurrent generation of their corresponding devices (Figure 2). The kinetics of the delayed exciplex emission in the microsecond timescale can be employed as an optical probe for monitoring the depletion of free charge density that has been created after exciton dissociation. The emissive bimolecular recombination is expected to accelerate with the increase of charge concentration in the systems and with the increase of the recombination coefficient. Previous results have shown that the magnitude of PL quenching in the F8BT:PDI system positively correlates with the device photocurrent[42] and therefore with the initial number of free charges in the photoactive layer. Based on these findings, a first estimation on the initial number of photogenerated charges in the as-spun and annealed F8BT:PDI and PIF8BT:PDI systems is possible based on the PCT-induced PL quenching measurements (Figure 3d). After thermal annealing of the F8BT:PDI blend, the concentration of the charges is reduced (reduced PL quenching efficiency) whereas the delayed luminescence kinetics are decelerated (reduced power law exponents, see Table 1). In contrast, after thermal annealing of the PIF8BT:PDI blend, the concentration of the charges is reduced (reduced PL quenching efficiency) but the delayed luminescence kinetics are accelerated (increased power law exponents, see Table 1). We therefore suggest that annealing does not severely affect the recombination coefficient in the F8BT:PDI system but it increases the recombination coefficient in the PIF8BT:PDI system. Despite the inferred increase in the recombination rate constant in the annealed PIF8BT:PDI layer, the observed increase in the EQE of the corresponding device suggests a beneficial effect of thermal treatment on the device performance. Table 1 shows that the power-law exponent is increased by more than 50%, correlating well with the increase in short-circuit photocurrent for the corresponding device. Similarly, in the case of the F8BT:PDI layer the decreased exponent of the power-law decay of the delayed CT-state fluorescence on annealing is in line with a reduced short-circuit photocurrent for the corresponding device. These correlations suggest that the device photocurrent and consequently the charge transport properties are not directly linked to the recombination coefficient of the rate law that dictates the charge recombination reaction in the PDI-based blends, but rather to the overall order of the rate law of this reaction. Our findings are in agreement with previous transient spectroscopic studies of non-geminate charge recombination that have shown a positive correlation between the order of charge recombination kinetics, the charge transport properties, and the photocurrent generation in fullerene-based OPV systems.[52–54]

We have found that the decay kinetics of the delayed exciplex emission accelerate with increasing excitation power (see Supporting Information). It was shown previoulsy that the CT intensity of the F8BT:PDI system has a sublinear dependence on the excitation pulse energy,[17] and that the EQE of the F8BT:PDI devices are strongly dependent on reverse bias and active layer thickness.[51] Therefore, it appears that charge transport limits the device EQE of thick F8BT:PDI layers and it is conceivable that emissive non-geminate charge recombination involves trapped charges.[32,55]

Our proposal, that the delayed emissive recombination is trap-assisted, is further supported by the delayed fluorescence dynamics observed at low temperature for as-spin-coated F8BT:PDI blend films (**see** Table S1 in the Supporting Information). There is a clear deceleration of the power-law kinetics at 77 K. This is not the case for the annealed F8BT:PDI where, with respect to the room temperature kinetics, an increased carrier recombination rate is observed at 77 K. A similar increase is seen for both the as-spin-coated and annealed PIF8BT:PDI blend films. The observed acceleration of the delayed luminescence decay dynamics at low temperature requires further experimental investigation. At this stage we can only suggest a plausible explanation. The carrier mobility decreases significantly at low temperature so that the probability for Coulomb capture increases. Moreover the recombination of free charges is an exothermic process and an enhanced recombination of the charges is expected at low temperatures.[56] This could be the case if deep energetic traps are absent, so that the necessity for endothermic carrier detrapping can be neglected.

Finally it is worth mentioning that although the triplet state of PDI[57,58] lies at energies much lower than the energy of the emissive CT state of the studied polymer/PDI blends ($T_{PDI} \approx$ 1.2 eV, $E_{CT} \approx$ 1.8 eV), the EQE values of these PDI OPV systems can reach values as high as 20%.[51,59] This situation is in contrast to the models proposed for polymer/fullerene blends

that predict severe photocurrent losses when the fullerene triplet state lies at lower energy than the CT state, especially when charge-carrier mobility is low.[60,61] This difference in behaviour will be important to better understand in order to eventually provide general guidelines for materials selection.

4. Conclusions

In summary, we have studied the relationship between emissive non-geminate charge recombination and photocurrent generation efficiency in F8BT:PDI and PIF8BT:PDI OPV blend films. For the case of the F8BT:PDI system, thermal treatment at 90 °C results in an extensive phase separation of PDI from the F8BT matrix, in the crystallization of the PDI domains and in a reduction in the area of the F8BT/PDI interfaces, where both prompt exciton dissociation and non-geminate charge recombination occur. In contrast, thermal treatment of the PIF8BT:PDI blend results in only partially crystallized PDI domains, a lower degree of phase separation of the PDI from the PIF8BT matrix, and leads to more efficient prompt exciton dissociation and non-geminate charge recombination than in the case of F8BT:PDI. Both systems exhibit delayed exciplex luminescence in the microsecond timescale, the strength and the dynamics of which appear to correlate well with the photocurrent generation efficiency of the corresponding solar cell devices. In agreement with previous transient absorption spectroscopic studies of similar OPV systems, our results have shown that the value of the power law exponent of the delayed luminescence kinetics can be a useful parameter for validating the charge transport properties of OPV photoactive layers. We therefore suggest delayed luminescence spectroscopy as a suitable optical non-destructive probe for the correlation of non-geminate recombination kinetics with the charge transport capabilities in OPV systems.

Further structural studies are required to elucidate the different packing motifs in the two blends studied herein. Nevertheless, the time-integrated UV-Vis absorption, external quantum efficiency, steady state PL, and delayed luminescence spectroscopy data all support the notion that thermal treatment of the PIF8BT:PDI layer results in a layer structure where the PIF8BT and the PDI components remain relatively well-mixed.

Our results emphasize the importance of identifying the specific donor–acceptor interactions as well as the donor and acceptor local packing in OPV blends by thermal and structural means. Moreover, they suggest that delayed luminescence spectroscopy of OPV blend films can be a simple spectroscopic technique for the selection of processing protocols that lead to high-quality donor/acceptor interfaces and to blend layer microstructures that support efficient photocurrent generation.

5. Experimental Section

Materials: The protocol for the synthesis of PIF8BT has been described elsewhere.[17] The number average molecular mass $\overline{M}_n$ and the polydispersity (D) of F8BT and of PIF8BT were determined by gel permeation (size exclusion) chromatography (GPC), using PS as a standard, $\overline{M}_n$(PS) = 400 kD. We found $\overline{M}_n$(F8BT) = 171.3 kD, D(F8BT) = 1.84, $\overline{M}_n$ (PIF8BT) = 15.4 kD, and D(PIF8BT) = 2.48. The deduced $\overline{M}_n$ values are expected to be significant overestimates due to the rigid rod nature of the polymer backbones[62] but they give a reasonable comparative measure. F8BT was provided by the Sumitomo Chemical Company Ltd. and used as received. PDI was purchased from Sensient Technology and further purified by column chromatography fractionation.

Solution Preparation: Solutions of F8BT:PDI and PIF8BT:PDI containing polymer and PDI in a weight ratio of 40:60 were prepared in CHCl3 with a 7.5 mg mL^{-1} polymer mass concentration. The 60 wt% PDI content was chosen according to the previously optimized F8BT:PDI formulation.[42]

Thin Film and Device Fabrication: Thin films of the F8BT:PDI and PIF8BT:PDI blends were prepared by spin-coating. Reference blend films of PDI in PS were prepared in an identical fashion. Bulk heterojunction devices were prepared for the F8BT:PDI and PIF8BT:PDI blends with as-spin-coated, annealed at 90 °C, and annealed at 120 °C photoactive layers. In all cases device annealing took place in a N_2-filled glovebox for a period of 15 min after cathode deposition. The device structures comprised glass/ITO/poly(ethylene)dioxythiophene:poly(styrene) sulphonate (PEDOT:PSS)/polymer donor:PDI acceptor blend/Al.[42]

Device Characterization: The external quantum efficiency (EQE) characterization of all devices was performed under the protection of an N_2 atmosphere. The light output from a Xe lamp was monochromated by a Digichrom 240 monochromator and the short-circuit device photocurrent was monitored by a Kethley electrometer as the monochromator was scanned. A calibrated Si photodiode (818-UV Newport) was used as a reference in order to determine the intensity of the light incident on the device, allowing the EQE spectrum to be deduced.

Photophysical Characterization: UV-vis absorption spectra of all blend films were recorded with a Jasco UV-vis spectrophotometer. Time-integrated and time-gated delayed luminescence (DL) measurements of the blend films were performed as previously described.[17] DL measurements were performed at 77 K with the use of a home-built liquid N_2 cryostat. Photoluminescence quantum yield (PLQY) measurements on the F8BT and PIF8BT films on quartz substrates were performed as previously described.[63]

Supporting Information

Supporting Information is available from the Wiley Online Library or from the author.

Acknowledgements

The authors thank the Royal Society for financial support (International Travel Grant TG091471). V.K. thanks the DFG for financial support in the framework of the IRTG 1404: Self-organized Materials for Optoelectronics. F.L. acknowledges Max Planck Research Group funding from the Max Planck Society. D.D.C.B. thanks the Sumitomo Chemical Company Ltd. for providing the F8BT polymer used in this study.

Received: November 26, 2011
Published online: March 15, 2012

[1] M. A. Green, K. Emery, Y. Hishikawa, W. Warta, *Prog. Photovoltaics Res. Appl.* **2011**, *19*, 84.
[2] S. C. Price, A. C. Stuart, L. Yang, H. Zhou, W. You, *J. Am. Chem. Soc.* **2011**, *133*, 4625.
[3] F. He, W. Wang, W. Chen, T. Xu, S. B. Darling, J. Strzalka, Y. Liu, L. Yu*J. Am. Chem. Soc.* **2011**, *133*, 3284.
[4] T.-T. Chu, J. Lu, S. Beaupre, Y. Zhang, J.-R Pouliot, S. Wakim, J. Zhou, M. Leclerc, Z. Li, J. Ding, Y. Tao, *J. Am. Chem. Soc.* **2011**, *133*, 4250.
[5] D. Veldman, O. Ipek, S. C. J. Meskers, J. Sweelssen, M. M. Koetse, S. C. Veenstra, J. M. Kroon, S. S. van Bavel, J. Loos, R. A. J. Janssen, *J. Am. Chem. Soc.* **2008**, *130*, 7721.

[6] P. E. Keivanidis, T. M. Clarke, S. Lilliu, T. Agostinelli, J. Emyr Macdonald, J. R. Durrant, D. D. C. Bradley, J. Nelson, *J. Phys. Chem. Lett.* **2010**, *1*, 734.
[7] I. A. Howard, R. Mauer, M. Meister, F. Laquai, *J. Am. Chem. Soc.* **2010**, *132*, 14866.
[8] A. C. Morteani, P. Sreearunothai, L. M. Herz, R. H. Friend, C. Silva, *Phys. Rev. Lett.* **2004**, *92*, 247402.
[9] T. Offermans, P. A. van Hal, S. C. J. Meskers, M. M. Koetse, R. A. J. Janssen, *Phys. Rev. B* **2005**, *72*, 045213.
[10] M. A. Loi, S. Toffanin, M. Muccini, M. Forster, U. Scherf, M. Scharber, *Adv. Funct. Mater.* **2007**, *17*, 2111.
[11] J. J. Benson-Smith, J. Wilson, C. Dyer-Smith, K. Mouri, S. Yamaguchi, H. Murata, J. Nelson, *J. Phys. Chem. B* **2009**, *113*, 7794.
[12] S. Inal, M. Schubert, A. Sellinger, D. Neher, *J. Phys. Chem. Lett.* **2010**, *1*, 982.
[13] K. Tvingstedt, K. Vandewal, Z. Fengling, O. Inganäs, *J. Phys. Chem. C* **2010**, *114*, 21824.
[14] C. Dyer-Smith, J. J. Benson-Smith, D. D. C. Bradley, H. Murata, W. J. Mitchell, S. E. Shaheen, S. A. Haque, J. Nelson, *J. Phys. Chem. C* **2009**, *113*, 14533.
[15] P. Panda, D. Veldman, J. Sweelssen, J. J. A. M. Bastiaansen, B. M. W. Langeveld-Vos, S. C. J. Meskers, *J. Phys. Chem. B* **2007**, *111*, 5076.
[16] J. J. Benson-Smith, L. Goris, K. Vandewal, K. Haenen, J. V. Manca, D. Vanderzande, D. D. C. Bradley, J. Nelson, *Adv. Funct. Mater.* **2007**, *17*, 451.
[17] P. E. Keivanidis, V. Kamm, C. Dyer-Smith, W. Zhang, F. Laquai, I. McCulloch, D. D. C. Bradley, J. Nelson, *Adv. Mater.* **2010**, *22*, 5183.
[18] K. Vandewal, A. Gadisa, W. D. Oosterbaan, S. Bertho, F. Banishoeib, I. Van Severen, L. Lutsen, T. J. Cleij, D. Vanderzande, J. Manca, *Adv. Funct. Mater.* **2008**, *18*, 2064.
[19] K. Vandewal, K. Tvingstedt, A. Gadisa, O. Inganäs, J. V. Manca, *Nat. Mater.* **2009**, *8*, 904.
[20] C. Deibel, T. Strobel, V. Dyakonov, *Adv. Funct. Mater.* **2010**, *22*, 4097.
[21] I. A. Howard, F. Laquai, *Macromol. Chem. Phys.* **2010**, *211*, 2063.
[22] J. Lee, K. Vandewal, S. R. Yost, M. E. Bahlke, L. Goris, M. A. Baldo, J. V. Manca, T. Van Voorhis, *J. Am. Chem. Soc.* **2010**, *132*, 11878.
[23] M. Hallermann, E. Da Como, J. Feldmann, M. Izquierdo, S. Filippone, N. Martín, S. Jüchter, E. von Hauff, *Appl. Phys. Lett.* **2010**, *97*, 023301.
[24] A. Gonzalez-Rabade, A. C. Morteani, R. H. Friend, *Adv. Mater.* **2009**, *21*, 3924.
[25] F. C. Jamieson, T. Agostinelli, H. Azimi, J. Nelson, J. R. Durrant, *J. Phys. Chem. Lett.* **2010**, *1*, 3306.
[26] M. Lenes, M. Morana, C. J. Brabec, P. W. M. Blom, *Adv. Funct. Mater.* **2009**, *19*, 1106.
[27] D. J. D. Moet, M. Lenes, M. Morana, H. Azimi, C. J. Brabec, P. W. M. Blom, *Appl. Phys. Lett.* **2010**, *96*, 213506.
[28] a) A.W. Hains, Z. Q. Liang, M. A. Woodhouse, B. A. Gregg, *Chem. Rev.* **2010**, *110*, 6689; b) B. Walker, C. Kim, T.-Q. Nguyen, *Chem. Mater.* **2011**, *23*, 470; c) J. E. Antony, *Chem. Mater.* **2011**, *23*, 583.
[29] X. Zhan, A. Faccetti, S. Barlow, T. J. Marks, M. A. Ratner, M. R. Wasielewski, S. R. Marder, *Adv. Mater.* **2011**, *23*, 268.
[30] P. E. Schwenn, K. Gui, A. M. Nardes, K. B. Krueger, K. H. Lee, K. Mutkins, H. Rubinstein-Dunlop, P. E. Shaw, N. Kopidakis, P. L. Burn, P. Meredith, *Adv. Energy Mater.* **2011**, *1*, 73.
[31] S. Di Motta, F. Negri, D. Fazzi, C. Castiglioni, E. V. Canesi, *J. Phys. Chem. Lett.* **2010**, *1*, 3334.
[32] J. J. Dittmer, E. A. Marseglia, R. H. Friend, *Adv. Mater.* **2000**, *12*, 1270.
[33] L. Schmidt-Mende, A. Fechtenkotter, K. Müllen, E. Moons, R. H. Friend, J. D. MacKenzie, *Science* **2001**, *293*, 1119.
[34] J. L. Li, F. Dierschke, J. S. Wu, A. C. Grimsdale, K. Müllen, *J. Mater. Chem.* **2006**, *16*, 96.
[35] M. Sommer, S. Huttner, U. Steiner, M. Thelakkat, *Appl. Phys. Lett.* **2009**, *95*, 183308.
[36] S. Shoaee, T. M. Clarke, C. Huang, S. Barlow, S. R. Marder, M. Heeney, I. McCulloch, J. R. Durrant, *J. Am. Chem. Soc.* **2010**, *132*, 12919.
[37] V. Kamm, B. Glauco, I. A. Howard, W. Pisula, A. Mavrinskiy, C. Li, K. Müllen, F. Laquai, *Adv. Energy Mater* **2011**, *1*, 297.
[38] J. A. Mikroyannidis, M. M. Stylianakis, G. D. Sharma, P. Balraju, M. S. Roy, *J. Phys. Chem. C* **2009**, *113*, 7904.
[39] G. D. Sharma, P. Balraju, J. A. Mikroyannidis, M. M. Stylianakis, *Sol. Energy Mater. Sol. Cells* **2009**, *93*, 2025.
[40] G. D. Sharma, P. Suresh, J. A. Mikroyannidis, M. M. Stylianakis, *J. Mater. Chem.* **2010**, *20*, 561.
[41] S. Shoaee, Z. An, X. Zhang, S. Barlow, S. R. Marder, W. Duffy, M. Heeney, I. McCulloch, J. R. Durrant, *Chem. Commun.* **2009**, *36*, 5445.
[42] P. E. Keivanidis, I. A. Howard, R. H. Friend, *Adv. Funct. Mater.* **2008**, *18*, 3189.
[43] P. E. Keivanidis, F. Laquai, I. A. Howard, R. H. Friend, *Adv. Funct. Mater.* **2011**, *21*, 1355.
[44] I. A. Howard, F. Laquai, P. E. Keivanidis, R. H. Friend, N. C. Greenham, *J. Phys. Chem. C* **2009**, *113*, 21225.
[45] Y. Yi, V. Coropceanu, J. L. Bredas, *J. Mater. Chem.* **2011**, *21*, 1479.
[46] R. W. Collins, W. Paul, *Phys. Rev. B* **1982**, *25*, 5263.
[47] J. Singh, *J. Non-Cryst. Solids* **2006**, *352*, 1160.
[48] A. C. Morteani, R. H. Friend, C. Silva, *Chem. Phys. Lett.* **2004**, *391*, 81.
[49] V. R. Nikitenko, D. Hertel, H. Bässler, *Chem. Phys. Lett.* **2001**, *348*, 89.
[50] S. Gelinas, O. Pare-Labrose, C.-N. Brosseau, S. Albert-Seifried, C. R. McNeill, K. R. Kirov, I. A. Howard, R. Leonelli, R. H. Friend, C. Silva, *J. Phys. Chem. C* **2011**, *115*, 7114.
[51] P. E. Keivanidis, P. K. H. Ho, R. H. Friend, *Adv. Funct. Mater.* **2010**, *20*, 3895.
[52] J. Nelson, *Phys. Rev. B* **2003**, *67*, 155209.
[53] J. Nelson, S. A. Choulis, J. R. Durrant, *Thin Solid Films* **2004**, *508*, 451.
[54] M. A. Faist, P. E. Keivanidis, S. Foster, P. H. Wobkenberg, T. D. Anthopoulos, D. D. C. Bradley, J. R. Durrant, J. Nelson, *J. Polym. Sci., Part B: Polym. Phys.* **2011**, *49*, 45.
[55] A. Baumann, T. J. Savenije, D. H. K. Murthy, M. Heeney, V. Dyakonov, C. Deibel, *Adv. Funct. Mater.* **2011**, *21*, 1687.
[56] S. C. J. Meskers, H. P. J. M. Dekkers, *J. Phys. Chem. A* **2001**, *105*, 4589.
[57] F. N. Castellano, S. Goeb, A. A. Rachford, *J. Am. Chem. Soc.* **2008**, *130*, 2766.
[58] W. E. Ford, P. V. Kamat, *J. Phys. Chem.* **1987**, *91*, 6373.
[59] P. E. Keivanidis, N. C. Greenham, H. Sirringhaus, R. H. Friend, J. C. Blakesley, R. Speller, T. Agostinelli, M. Campoy-Quiles, D. D. C. Bradley, J. Nelson, *Appl. Phys. Lett.* **2008**, *92*, 023304.
[60] D. Veldman, S. C J. Meskers, R. A. J. Janssen, *Adv. Funct. Mater.* **2009**, *19*, 1939.
[61] C. Dyer-Smith, L. X. Reynolds, A. Bruno, D. D. C. Bradley, S. A. Haque, J. Nelson, *Adv. Funct. Mater.* **2010**, *20*, 2701.
[62] M. Grell, D. D. C. Bradley, X. Long, T. Chamberlain, M. Inbasekaran, E. P. Woo, M. Soliman, *Acta Polym.* **1998**, *49*, 439.
[63] J. C. deMello, H. F. Wittmann, R. H. Friend, *Adv. Mater.* **1997**, *9*, 230.